Geophysical Research Letters

RESEARCH LETTER
10.1029/2019GL085788

Key Points:
- Two ice-constraining approaches in coupled models (albedo and nudging) to study the climate responses of future ice loss are evaluated
- Given the same seasonal cycle of ice loss, ice albedo reduction and ice-flux nudging generate very similar global climate responses
- Ice albedo reduction underestimates projected winter sea ice loss and thus its impacts, with implications for coordinated model experiments

Supporting Information:
- Supporting Information S1

Correspondence to:
L. Sun,
lantao.sun@colostate.edu

Citation:
Sun, L., Deser, C., Tomas, R. A., & Alexander, M. (2020). Global coupled climate response to polar sea ice loss: Evaluating the effectiveness of different ice-constraining approaches. *Geophysical Research Letters*, *47*, e2019GL085788. https://doi.org/10.1029/2019GL085788

Received 10 OCT 2019
Accepted 15 JAN 2020
Accepted article online 21 JAN 2020

Global Coupled Climate Response to Polar Sea Ice Loss: Evaluating the Effectiveness of Different Ice-Constraining Approaches

Lantao Sun[1], Clara Deser[2], Robert A. Tomas[2], and Michael Alexander[3]

[1]Department of Atmospheric Science, Colorado State University, Fort Collins, CO, USA, [2]National Center for Atmospheric Research, Boulder, CO, USA, [3]NOAA Earth System Research Laboratory Physical Science Division, Boulder, CO, USA

Abstract Coupled ocean-atmosphere models have been utilized to investigate the global climate response to polar sea ice loss using different approaches to constrain ice concentration and thickness. The goal of this study is to compare two commonly used methods within a single model framework: ice albedo reduction, which is energy conserving, and ice-flux nudging, which is not energy conserving. The two approaches generate virtually identical equilibrium global climate responses to the same seasonal cycle of sea ice loss. However, while ice-flux nudging is able to control the sea ice state year-round, albedo reduction is most effective during summer and lessens the effects of climate change in winter due to the underestimation of sea ice loss. These evaluations have implications for the Polar Amplification Model Intercomparison Project (PAMIP), which proposes a set of coordinated coupled model experiments but without a defined protocol on how to constrain sea ice.

Plain Language Summary What does polar amplification mean for global climate? This question has been addressed by using different arbitrary methods to isolate melting of Arctic and/or Antarctic sea ice in coupled ocean-atmosphere modeling experiments. However, these experiments sometimes obtained different answers. It is still unclear whether the divergent results arise from models' structural differences or from the different methods used to melt sea ice. In this study, two commonly used approaches (albedo reduction and nudging) are applied to a single climate model to generate the same seasonal cycle of ice loss and polar amplification. Nearly identical responses are found, including slowing down the thermohaline circulation in the Atlantic Ocean, weakened westerly winds over high latitudes, increased precipitation over the west coast of North America associated with a deepened Aleutian Low, and tropical upper tropospheric warming. However, ice albedo reduction is found to be ineffective in winter, unlike nudging, which can control sea ice year-round. We therefore recommend nudging to be adopted for the Polar Amplification Model Intercomparison Project (PAMIP) coupled experiments.

1. Introduction

The warming Arctic and associated melting of the ice cap are among the most prominent features of anthropogenic climate change. Understanding the global consequences of observed and projected Arctic sea ice loss is an area of active research with many outstanding questions. Empirical studies suggest a connection between Arctic sea ice loss and cold air outbreaks over Eurasia (e.g., Cohen et al., 2013; Francis & Vavrus, 2012; Kug et al., 2015; Overland et al., 2011), although the direction of causality is under debate (Blackport et al., 2019; Blackport & Screen, 2019; Collow et al., 2018; Kretschmer et al., 2016; McCusker et al., 2016; Mori et al., 2014; Mori et al., 2019; Ogawa et al., 2018; Peings, 2019; Perlwitz et al., 2015; Sun et al., 2016). Modeling studies targeting future sea ice loss (i.e., isolating the sea ice change seen in coupled model experiments with increasing greenhouse gases) have shown the importance of ocean-atmosphere coupling, not only for magnifying the extratropical atmospheric response but also for communicating the response into the tropics and Southern Hemisphere (Deser et al., 2015, 2016; Blackport & Kushner, 2016, 2017, 2018; Tomas et al., 2016; Oudar et al., 2017; Cvijanovic et al., 2017; Smith et al., 2017; Sun et al., 2018; Wang et al., 2018; Liu & Fedorov, 2019). While models agree on the general characteristics of the atmospheric and oceanic responses to Arctic sea ice loss, such as a weakening of the westerlies on the poleward flank of the jet stream and a reduction in the strength of the Atlantic meridional overturning circulation

(AMOC), regional climate responses are less consistent (Hay et al., 2018; Screen et al., 2018). The extent to which these discrepancies arise from structural differences across models (i.e., model physics and resolution) or from differences in experimental design (location of sea ice loss and methodology) has not been documented. Thus, a coordinated experimental protocol is needed to properly compare model simulations (Smith et al., 2019).

In the aforementioned coupled modeling studies, sea ice has been manipulated in different ways by modifying the surface energy budget. The two most common approaches are (1) albedo reduction, which includes ice and/or snow parameter adjustments (Bitz et al., 2006; Blackport & Kushner, 2016, 2017; Blackport & Screen, 2019; Cvijanovic et al., 2017; Graversen & Wang, 2009; Liu et al., 2019; Liu & Fedorov, 2019; Scinocca et al., 2009; Winton, 2008); and (2) "ghost flux" (Deser et al., 2015; Oudar et al., 2017) or similar "ice-flux" (McCusker et al., 2017; Sun et al., 2018) nudging schemes, in which an additional surface heat flux term is added to the sea ice module (the term "ghost flux" refers to the fact that this additional energy is invisible to other components of the model: Deser et al., 2015; Screen et al., 2018). Albedo reduction conserves energy but is only effective during the sun-lit portion of the year. By contrast, ghost flux and ice-flux nudging do not conserve energy but are effective in adjusting sea ice year-round. Other methods have also been used to melt sea ice, such as sea surface temperature (SST) relaxation or abrupt CO_2 quadrupling at high latitudes (Stuecker et al., 2018; Yoshimori et al., 2018). However, these approaches introduce additional forcing perturbations besides sea ice loss and thus target the response to high-latitude warming in general instead of sea ice loss in particular.

It is still unclear the extent to which the coupled climate response to sea ice loss is sensitive to these different approaches, since there has been no attempt to compare different approaches within a single modeling framework. Ghost flux and ice-flux nudging, for instance, have been criticized for not conserving energy. While this flux is only prescribed to the ice model (Deser et al., 2015; Sun et al., 2018), the artificial flux could exert an additional influence on the ocean and/or atmosphere, thus making it difficult to determine whether the response originates solely from sea ice change (Cvijanovic et al., 2017). However, consistent extratropical atmospheric responses to future Arctic sea ice loss have been found for both ghost flux and albedo reduction methodologies (Blackport & Kushner, 2016, 2017; Deser et al., 2015; Screen et al., 2018), implying energy conservation might not be that important. Nevertheless, one cannot rule out the possibility that there could still be some sensitivity to the method of sea ice melting, especially in remote regions such as the tropics. For example, the albedo reduction method (Liu & Fedorov, 2019) and the ghost/ice-flux nudging method (Deser et al., 2015; Tomas et al., 2016; Wang et al., 2018; Sun et al., 2018) yield somewhat different patterns of tropical SST and precipitation responses. Without further investigations, it is not obvious whether the different responses are due to the ice-constraining approach or other factors (e.g., model physics, resolution, and sea ice forcing).

A coordinated set of coupled ocean-atmosphere model experiments has been proposed as part of the Polar Amplification Model Intercomparison Project (PAMIP) to investigate the global climate response to Arctic and Antarctic sea ice loss on decadal and centennial timescales (Smith et al., 2019). In these experiments, polar sea ice will be artificially decreased without altering greenhouse gas (GHG) concentrations so as to differentiate its effect on the global climate system from other aspects of anthropogenic climate change. However, there is as yet no defined protocol on how to constrain sea ice in models, and it is still unclear which approach(es) should be used in PAMIP.

The goal of this study is to compare two approaches for constraining sea ice using a single coupled model. To that end, we present a pair of 360-year climate model experiments with approximately the same Arctic and Antarctic sea ice loss but achieved through albedo reduction and ice-flux nudging, respectively. We examine the sensitivity of the global atmospheric and oceanic responses to these two methods and evaluate the effectiveness of the different ice-constraining approaches for achieving the desired sea ice state. Lastly, based on the findings, we provide recommendations on experimental protocol for PAMIP.

2. Model Experiment Design

We build upon an existing set of constrained sea ice simulations (Deser et al., 2015) with the fully coupled Community Climate System Model Version 4 (CCSM4; Gent et al., 2011). All experiments are conducted for 360 years with the first 100 years discarded as spin-up, and the radiative forcings are

fixed at the year 2000. In the control experiment (hereafter "CONTROL"), Arctic and Antarctic sea ice concentrations and thicknesses approximate late 20th century (1980–1999) conditions simulated by a five-member ensemble of CCSM4 historical simulations (There is slight constraining on the Arctic sea ice; see Deser et al., 2015. Whether there is ice constraining or not in the control run should not substantially affect our conclusion, because the climate response is calculated by subtracting the same climatology). In the albedo experiment (hereafter "ALBEDO"), ice and snow albedo values are lowered to achieve a September Arctic sea ice extent that is close to the 2080–2099 climatology of a five-member ensemble of CCSM4 Representative Concentration Pathway 8.5 (RCP8.5) simulations. This is done by justifying the tuning parameters for snow (r_snw = −10.0; rsnw_melt_in = 3,000) and ice (r_ice = −4.0), similar to Blackport and Kushner (2016). It is important to note that the sea ice extent in ALBEDO greatly underestimates the sea ice loss in RCP8.5 during the winter months, a point we shall return to in section 3. Finally, in the ghost flux simulation (denoted "GHOST_F"), an additional seasonally varying downward energy flux is added to the sea ice module in the Arctic to achieve a seasonal cycle of ice concentration and thickness that is close to the 2080–2099 climatology of the five-member ensemble of CCSM4 RCP8.5 simulations.

We also conduct a new 360-year simulation (denoted "NUDGE") in which we use ice flux nudging to achieve approximately the same seasonal cycle of sea ice concentration and thickness as in ALBEDO. In this way, we can directly compare the global climate responses in the two experiments, since their sea ice loss is nearly identical. The ice flux nudging scheme developed for CCSM4 does not directly nudge the sea ice concentration as in Smith et al. (2017). Instead, it constrains ice volume by modifying the surface energy flux within the ice model (Knutson, 2003; McCusker et al., 2017; Sun et al., 2018). At each time step, a time-varying flux is calculated by

$$Q_{\mathrm{flux}} = \frac{L_{\mathrm{ice}} D_{\mathrm{ice}} (C_{\mathrm{ice}} h_{\mathrm{ice}} - C_{\mathrm{ice\_t}} h_{\mathrm{ice\_t}})}{\tau_{\mathrm{ice}}}, \quad (1)$$

where L_{ice} is the latent heat of fusion (3.34×10^5 J kg^{-1}), D_{ice} is the density of ice (905 kg m^{-3}), C_{ice} is the sea ice concentration (%), h_{ice} is the sea ice thickness (m), C_{ice_t} is the target sea ice concentration, h_{ice_t} is the target sea ice thickness, and τ_{ice} is the relaxation times. This flux is applied to the bottom of the ice, thereby adjusting the ice concentration and thickness toward the target values. While energy is not conserved, the water mass budget is conserved, which is desirable because the freshwater flux is important for the AMOC response (Liu et al., 2019).

A crucial factor for the ice flux nudging scheme is the selection of nudging timescale. When a value of 60 days is used as recommended by PAMIP (Smith et al., 2019), the sea ice area in both hemispheres is overestimated compared to the target ALBEDO simulation (supporting information Figure S1). To improve upon this, three additional simulations were run with nudging timescales of 1, 5, and 10 days. For both the Arctic and Antarctic, the overestimation of sea ice area lessens when the nudging timescale decreases (Figure S2) and eventually changes to an underestimation for 1-day nudging. In addition, there is slight downward drift in sea ice area over the 360-year simulation, especially in the Antarctic, and this drift appears for both the 1- and 10-day nudging timescales. This is possibly due to the feedback of extratropical SST warming as a result of sea ice loss. Based on these sensitivity tests, we chose 10 days for the damping timescale. Similar results are found when the sensitivity tests are evaluated using on sea ice volume instead of sea ice area (not shown).

The September and March sea ice concentrations and sea ice area for the CONTROL, ALBEDO, and NUDGE simulations are shown in Figure 1, and the corresponding sea ice thickness distributions are shown in Figure S3. There is a very close match between ALBEDO and NUDGE sea ice conditions when averaged over years 101–360: Their annual sea ice area difference is less than 0.1 million km^2, which is less than 5% of the polar sea ice loss relative to CONTROL.

The climate response to polar sea ice loss in each experiment is defined relative to the control simulation:

$$\Delta\mathrm{ALBEDO} = \mathrm{ALBEDO}–\mathrm{CONTROL}, \quad (2)$$

$$\Delta\mathrm{NUDGE} = \mathrm{NUDGE}–\mathrm{CONTROL}, \quad (3)$$

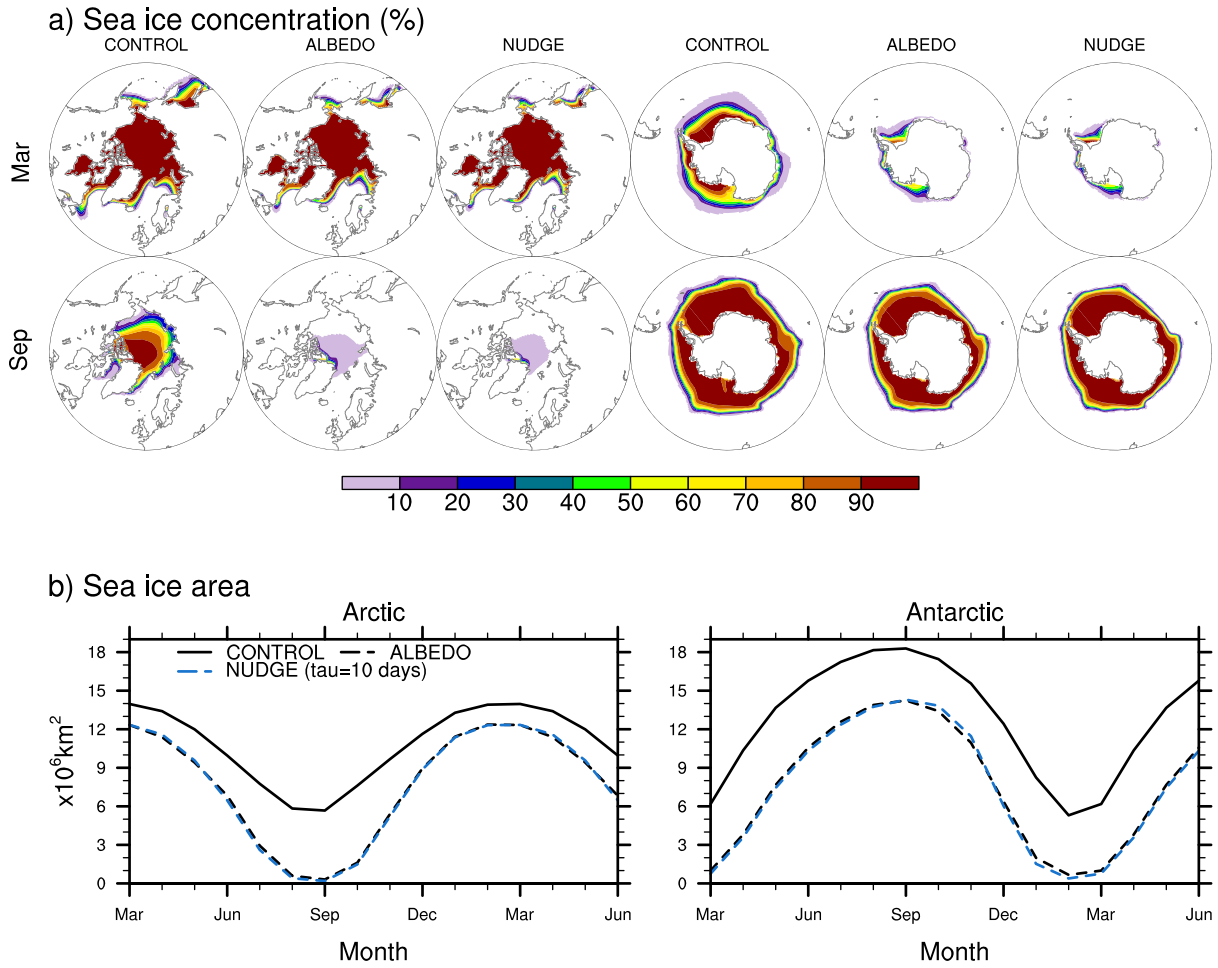

Figure 1. (a) March and September Arctic and Antarctic sea ice concentrations (%) in the CCSM4 CONTROL, ALBEDO, and NUDGE experiments. (b) Monthly Arctic (left) and Antarctic (right) sea ice area (10^6 km^2) in the CONTROL (solid black line), ALBEDO (dashed black line), and NUDGE experiments (nudging timescale of 10 days; dashed blue line). The months March–June are repeated for clarity.

$$\Delta\text{GHOST\_F} = \text{GHOST\_F} - \text{CONTROL}. \quad (4)$$

The March and September polar sea ice loss in ΔALBEDO, ΔNUDGE, and their difference are shown in Figure S4.

The statistical significance is evaluated using a two-sided Student's *t* test, and the number of degrees of freedom is calculated by taking into account the serial correlation (Zwiers & von Storch, 1995).

3. Results

The annual-mean global SST responses in ΔALBEDO (left), ΔNUDGE (middle), and their difference (right) are shown in Figures 2a–2c. Overall, these two experiments generate very similar responses, with a pattern correlation above 0.99 and root-mean-square (RMS) difference of 0.04 °C. SSTs increase everywhere except directly east of northern Japan and along the northern flank of the Gulf Stream, with maximum warming (1–2 °C) in regions of sea ice loss. The tropical oceans warm by 0.4–0.6 °C, with a maximum along the equator especially in central and eastern Pacific. The magnitudes of AMOC weakening are also comparable (Figure S5), and the structures of the AMOC response are almost identical for two approaches (Figure S6).

The precipitation response is also very similar between the two experiments (Figures 2d and 2e; pattern correlation of 0.88 and RMS difference of 0.06 mm day^{-1}). Diminished sea ice enhances precipitation locally,

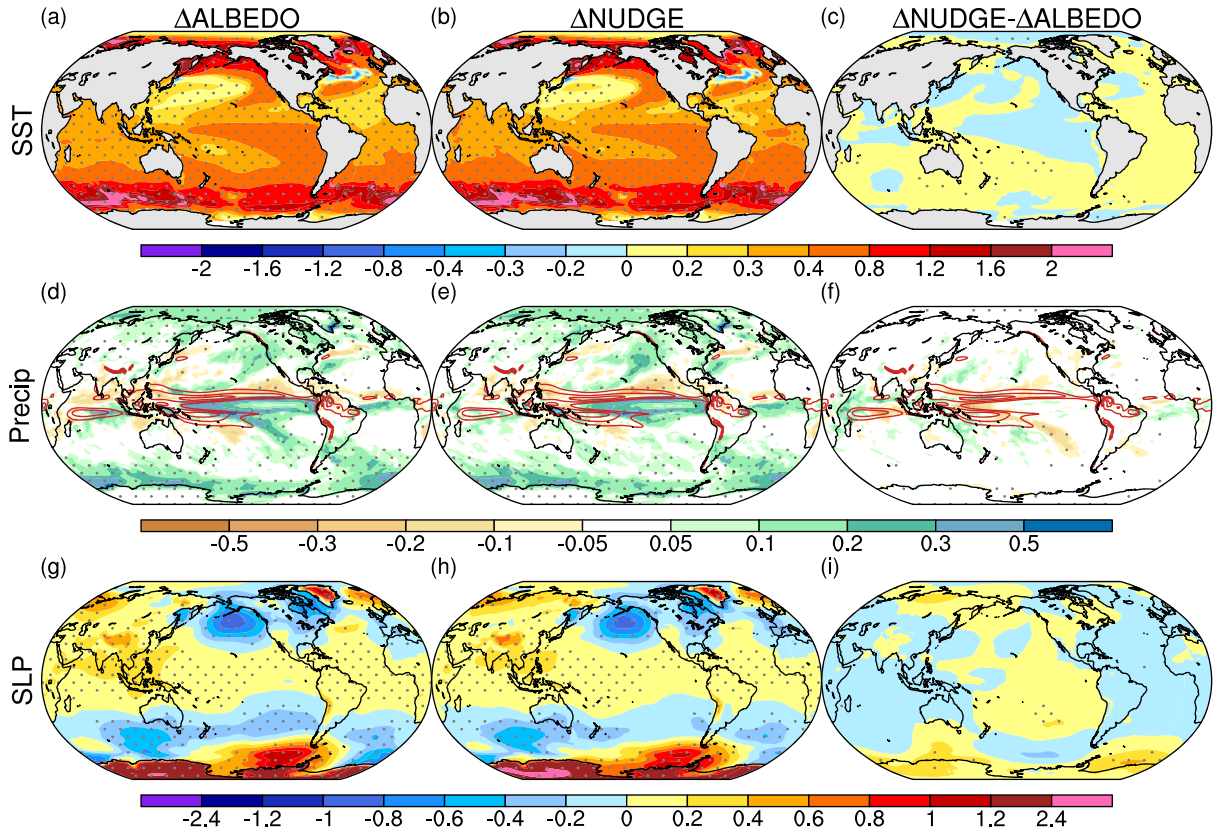

Figure 2. Annual (a, b, c) SST (°C), (d, e, f) precipitation (mm day^{-1}), and (g, h, i) sea-level pressure (hPa) responses in (left) ΔALBEDO, (middle) ΔNUDGE, and their difference (right). The red contour lines in the middle panel show the climatological precipitation (6, 8, and 10 mm day^{-1} isopleths) for context. Stippling denotes the 95% confidence level based on a two-sided Student's *t* test.

with slightly larger magnitude in the Antarctic compared to the Arctic. In the tropical Pacific, there are two zonally oriented bands of enhanced precipitation on either side of the equator across much of the basin, flanked on their poleward sides by negative precipitation anomalies. This implies an equatorward shift and intensification of the climatological ITCZ (contours). Precipitation also increases near the equator over the Atlantic. There are some differences in the small-scale features and magnitudes of the tropical precipitation response in ΔALBEDO and ΔNUDGE, but these are mostly statistically insignificant (Figure 2f). When zonally averaged, the responses are nearly identical at each latitude (not shown).

The sea-level pressure responses are also very similar in the two experiments (Figures 2g and 2h; pattern correlation of 0.97 and RMS difference of 0.08 hPa), with negative anomalies over eastern North America and positive anomalies over northern Eurasia, which is a robust feature across models (Hay et al., 2018; Screen et al., 2018). There is also a pronounced deepening of the Aleutian Low, and the associated counterclockwise circulation transports warm moist air on its eastern side leading to an increase in precipitation along the western United States and Canada (Figures 2d and 2e). This circulation change is largely due to teleconnections driven by tropical SST warming (Tomas et al., 2016) but may also partly result from the direct sea ice forcing (e.g., Deser et al., 2016; Sun et al., 2015) and extratropical SST warming (Blackport & Kushner, 2018). Sea-level pressure increases over Antarctica and decreases in the Southern Hemisphere midlatitudes, in agreement with other similar studies (e.g., Ayres & Screen, 2019; England et al., 2018).

Figure 3 shows the annual zonal-mean temperature and zonal wind responses in ΔALBEDO (left), ΔNUDGE (middle), and their difference (right) as a function of pressure and latitude, superimposed on the climatology (contours). Again, the features are broadly similar in the two experiments, and the differences are small and statistically insignificant. The temperature response is nearly symmetric about the equator, with strong polar amplification near the surface and in the tropical upper troposphere. It

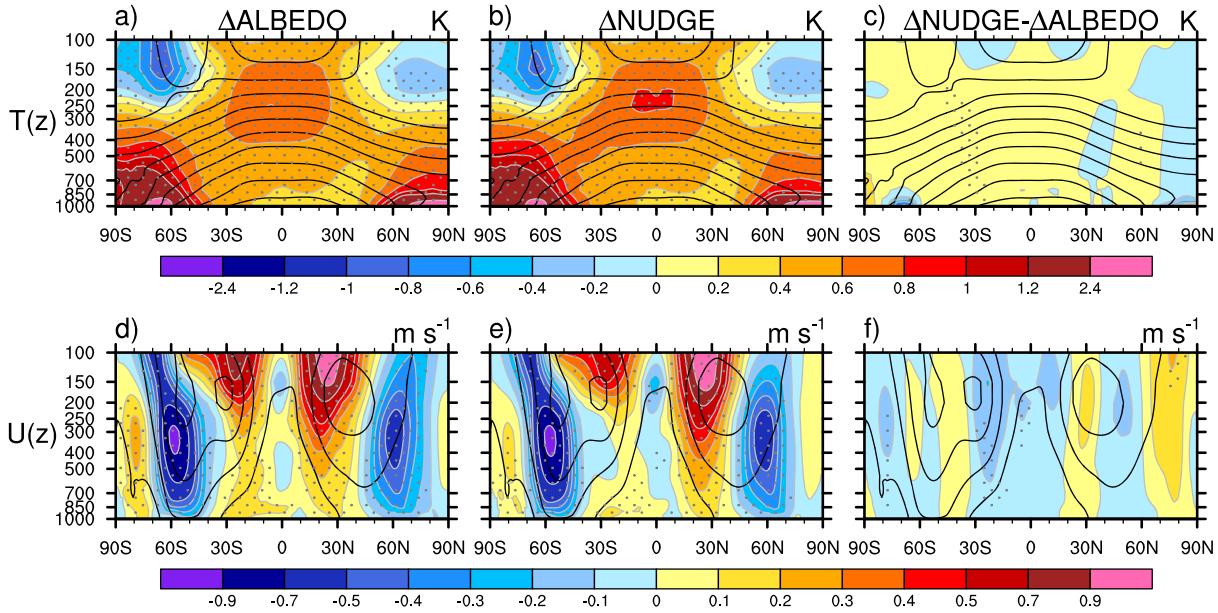

Figure 3. Annual zonal-mean (a, b, c) air temperature (°C) and (d, e, f) zonal wind (m s^{-1}) responses in (left) ΔALBEDO, (middle) ΔNUDGE, and their difference (right) as a function of pressure and latitude. The black contour lines denote the climatological values with an interval of 10°C for temperature and 10 m s^{-1} for zonal wind. Stippling denotes the 95% confidence level based on a two-sided Student's *t* test.

resembles the overall response to an increase in GHG, but with much-reduced amplitude: hence, the term "mini-global warming" (Deser et al., 2015). The extratropical stratosphere cools slightly (similar to Sun et al., 2018) with nearly the same magnitude in both ΔALBEDO and ΔNUDGE. Consistent with the temperature responses and thermal wind considerations, the zonal wind is reduced in the latitude bands 45–80°N and 40–70°S, with maxima at 60°N/S near 300 hPa, and increased in the subtropical lower stratosphere in both hemispheres.

We also examine the seasonality by averaging the responses over extended boreal winter (October–March) and summer (April–September) seasons, as shown in Figures S7–S10. Deepening of the Aleutian Low and increased precipitation over the western coast of North America occur mainly in the boreal winter. Weakening of the westerly winds near 60°N and 60°S is largest in the corresponding winter season of each hemisphere, consistent with seasonality of the polar warming. But more importantly, the differences between ΔALBEDO and ΔNUDGE are small and mostly statistically insignificant in either season.

As mentioned above, our ALBEDO simulations (and those of Blackport & Kushner, 2016, 2017) underestimate winter sea ice loss relative to RCP8.5. This is highlighted in Figure 4a, which compares the monthly sea ice area loss in ΔGHOST_F (red bars), in which the sea ice is nudged to the 2080–2099 state of the CCSM4 RCP8.5 simulations, with ΔALBEDO (blue bars) and ΔNUDGE (orange bars). The seasonal cycles of ice area loss are very similar in ΔALBEDO and ΔNUDGE, by design. However, they underestimate ice area loss in RCP8.5 in all months except September. In boreal winter (e.g., November, December, and January), the loss of Arctic ice is underestimated by as much as ~50%. While matching September sea ice as done here is arbitrary and one may choose larger albedo reduction to better match other seasons, the ineffectiveness of constraining sea ice in winter appears to be a common issue in previous studies using the albedo approach.

The underestimation of sea ice loss in ΔALBEDO compared to RCP8.5 can substantially affect the magnitudes of the local and remote responses. Figure 4b shows the monthly Arctic surface energy flux response (sum of sensible, latent, and longwave fluxes averaged over climatological March sea ice extent in CONTROL), where positive values denote upward flux anomalies. The energy entering the atmosphere is substantially underestimated in ΔALBEDO and ΔNUDGE compared to ΔGHOST_F, especially in winter when the peak flux response occurs. As a result, warming of the Arctic lower troposphere is substantially less in ΔALBEDO and ΔNUDGE compared to ΔGHOST_F (not shown, but see Deser et al., 2015 for

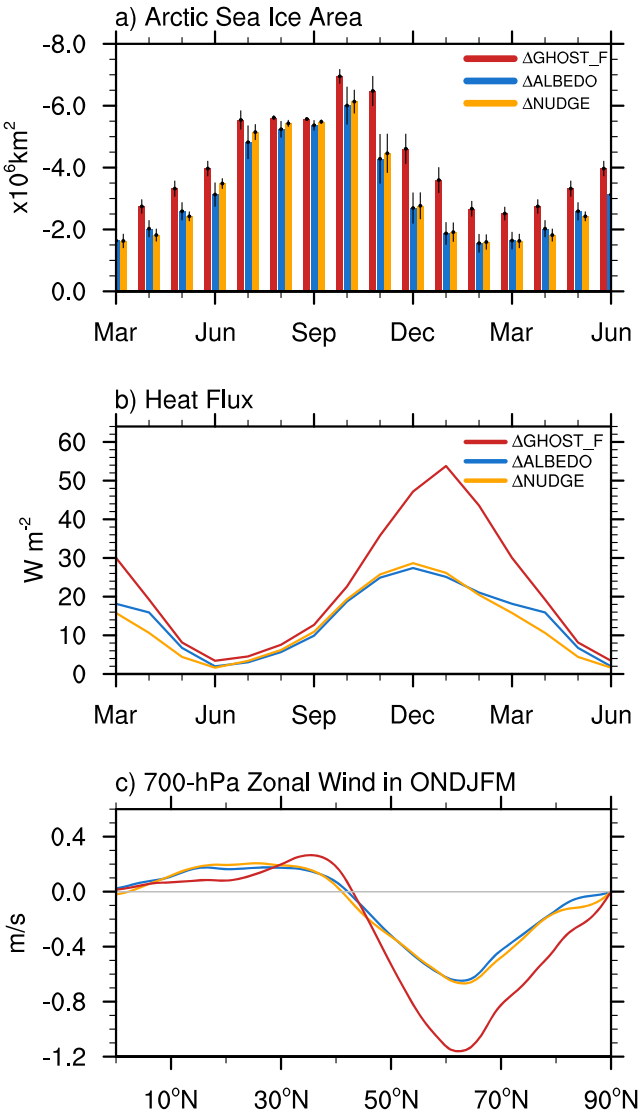

Figure 4. (a) Monthly Arctic sea ice area anomaly (10^6 km^2; note inverted scale) in ΔGHOST_F (red), ΔALBEDO (blue), and ΔNUDGE (orange) experiments. The months March–June are repeated for clarity. Error bars denote +/− one standard deviation. (b) Net surface heat flux response (sum of the turbulent and longwave radiative flux components, positive upward; W m^{-2}) to polar sea ice loss in ΔGHOST_F (red), ΔALBEDO (blue), and ΔNUDGE (orange). In (a) and (b), the months March–June are repeated for clarity. (c) The zonal-mean zonal wind response at 700 hPa averaged over October–March (m s^{-1}) in ΔGHOST_F (red), ΔALBEDO (blue), and ΔNUDGE (orange). Note that the seasonal cycle of Arctic sea ice area anomaly in ΔGhost_F is very similar to the ice loss in 2080–2099 relative to 1980–1999 in CCSM4 under historical and RCP8.5 radiative forcing.

temperature response in ΔGHOST_F). It is therefore not surprising that the decrease in zonal-mean zonal wind at 700 hPa during winter (October–March) over the latitude band 50–70°N is substantially smaller in ΔALBEDO and ΔNUDGE compared to ΔGHOST_F (Figure 4c). The magnitude of AMOC weakening is also underestimated in ΔALBEDO experiments (Figure S5).

4. Implications for Coordinated Experiments in PAMIP

Although PAMIP involves a coordinated set of coupled modeling experiments to investigate the response to sea ice loss, there are no formal recommendations on a common experimental protocol to be used for constraining sea ice. To fill this void, we have compared two methodologies using long (360 year) simulations with CCSM4, taking care to ensure that the sea ice loss in both hemispheres is nearly identical in the two approaches. Our results reveal that the two techniques result in virtually the same global atmospheric and oceanic responses, including (1) polar amplification and locally enhanced precipitation, (2) weakening of the AMOC, (3) equatorward displacement of the Pacific ITCZ, (4) deepening of the Aleutian Low and increased precipitation over the western United States and Canada, (5) "mini-global warming" signature in tropospheric temperatures, and (6) zonal wind deceleration near 60°N/S. All of these features are consistent with most previous coupled modeling studies on this topic (Deser et al., 2015, 2016; Tomas et al., 2016; Blackport & Kushner, 2016, 2017; Oudar et al., 2017; Wang et al., 2017; Sun et al., 2018; Hay et al., 2018; Blackport & Screen, 2019). Note that our findings are distinct from those of Cvijanovic et al. (2017) who found increased geopotential height over the North Pacific and decreased precipitation over the west coast of the United States in response to Arctic sea ice loss. They speculated that the disparity between their results and previous studies is due to the method used to constrain sea ice. Our results suggest that the disparity is more likely due to the inadequacy of the slab-ocean model configuration used in Cvijanovic et al. (2017) rather than the ice-constraining methodology.

Despite the consistency in response patterns, the ALBEDO experiment has been found to underestimate winter sea ice loss, and thus its local and remote impacts. This leads us to make some suggestions based on the effectiveness of the ice-constraining approaches to be used in the PAMIP coupled experiments. We acknowledge that all sea ice-constraining approaches are idealized, since sea ice loss is just one component of the response to increased GHG and is always tied to other changes. As a result, all sea ice-constraining approaches are imperfect (Smith et al., 2019). For example, in the ice-flux nudging experiments, sea ice has too little variability at interannual timescales compared to the albedo method (Figure S11) as does the associated interannual SST variability (Figure S12). In addition, the ice-flux nudging appears to have difficulty matching the sea ice in winter when the target sea ice becomes very thin (e.g., in the highly sensitive model such as Geophysical Fluid Dynamics Laboratory Coupled Model Version 3; Sun et al., 2018). Nevertheless, for the purpose of model intercomparison, a recommended experimental protocol will benefit the PAMIP community and enable better coordination among the model institutes performing the experiments.

Based on our findings, we recommend using the ghost flux or ice-flux nudging approaches in the PAMIP coupled experiments. These approaches are effective at constraining polar sea ice year-round and do not

appear to produce spurious responses. They can be compared directly to the atmosphere-only model experiments to isolate the role of ocean-atmosphere coupling (e.g., Deser et al., 2015, 2016) and can be more closely compared with other PAMIP coupled experiments because the ice forcing is approximately identical. We also emphasize that to properly constrain polar sea ice, both concentration and thickness need to be considered, and the global freshwater water budget needs to be conserved. These are vital for understanding the ocean response (e.g., AMOC and associated SST and sea surface salinity) to past and future sea ice loss.

If the model infrastructure is too complex to adopt ice nudging, albedo reduction can also provide useful information. However, one must bear in mind that this approach underestimates winter sea ice loss, and thus its local and remote effects especially in winter (which are driven by the concurrent winter ice loss: Sun et al., 2015; Blackport & Screen, 2019). A further consequence is that comparison with other PAMIP experiments will be more qualitative in nature. However, the pattern scaling approach developed by Blackport and Kushner (2017) and Hay et al. (2018) might be able to account for some of the sea ice differences, but with potential limitations due to its assumption of linearity.

Acknowledgments
We appreciate the constructive suggestions of the two anonymous reviewers. We also appreciate valuable discussions with Dave Bailey and Marika Holland (NCAR) in developing the CCSM4 ice-flux nudging technique, and suggestions from Jim Hurrell (CSU) and Matt Newman (CIRES/NOAA ESRL) and comments from participants at the PAMIP workshop in June 2019. LS is supported by Jim Hurrell's presidential chair startup funding at CSU. This project is partly supported by the NOAA Climate Program Office Earth System Modeling program. We would like to acknowledge high-performance computing support from Cheyenne provided by NCAR's Computational and Information Systems Laboratory, sponsored by the National Science Foundation. NCAR is sponsored by the National Science Foundation. Model data are available at https://zenodo.org/record/3479888#.XZ_PP-dKhBw.

References

Ayres, H., & Screen, J. A. (2019). Multimodel analysis of the atmospheric response to Antarctic sea ice loss at quadrupled CO_2. *Geophysical Research Letters*, *46*, 9861–9869. https://doi.org/10.1029/2019GL083653

Bitz, C. M., Gent, P. R., Woodgate, R. A., Holland, M. M., & Lindsay, R. (2006). The influence of sea ice on ocean heat uptake in response to increasing CO_2. *Journal of Climate*, *19*, 2437–2450. https://doi.org/10.1175/JCLI3756.1

Blackport, R., & Kushner, P. (2016). The transient and equilibrium climate response to rapid summertime sea ice loss in CCSM4. *Journal of Climate*, *29*, 401–417. https://doi.org/10.1175/JCLI-D-15-0284.1

Blackport, R., & Kushner, P. J. (2017). Isolating the atmospheric circulation response to Arctic sea ice loss in the coupled climate system. *Journal of Climate*, *30*(6), 2163–2185. https://doi.org/10.1175/JCLI-D-16-0257.1

Blackport, R., & Kushner, P. J. (2018). The role of extratropical ocean warming in the coupled climate response to Arctic sea ice loss. *Journal of Climate*, *31*(22), 9193–9206. https://doi.org/10.1175/JCLI-D-18-0192.1

Blackport, R., & Screen, J. A. (2019). Influence of Arctic sea ice loss in autumn compared to that in winter on the atmospheric circulation. *Geophysical Research Letters*, *46*, 2213–2221. https://doi.org/10.1029/2018GL081469

Blackport, R., Screen, J. A., van der Wiel, K., & Bintanja, R. (2019). Minimal influence of reduced Arctic sea ice on coincident cold winters in mid-latitudes. *Nature Climate Change*, *9*(9), 697–704. https://doi.org/10.1038/s41558-019-0551-4

Cohen, J. L., Jones, J. C., Furtado, J. C., & Tziperman, E. (2013). Warm Arctic, cold continents. *Oceanography*, *26*(4). https://doi.org/10.5670/oceanog.2013.70

Collow, T. W., Wang, W., & Kumar, A. (2018). Simulations of Eurasian winter temperature trends in coupled and uncoupled CFSv2. *Advances in Atmospheric Sciences*, *35*(1), 14–26. https://doi.org/10.1007/s00376-017-6294-0

Cvijanovic, I., Santer, B., Bonfils, C., Lucas, D. D., Chiang, J. C. H., & Zimmerman, S. (2017). Future loss of Arctic sea-ice cover could drive a substantial decrease in California's rainfall. *Nature Communications*, *8*(1), 1–10. https://doi.org/10.1038/s41467-017-01907-4

Deser, C., Sun, L., Tomas, R. A., & Screen, J. A. (2016). Does ocean coupling matter for the northern extratropical response to projected Arctic sea ice loss? *Geophysical Research Letters*, *43*, 2149–2157. https://doi.org/10.1002/2016GL067792

Deser, C., Tomas, R. A., & Sun, L. (2015). The role of ocean-atmosphere coupling in the zonal-mean atmospheric response to Arctic sea ice loss. *Journal of Climate*, *28*, 2168–2186. https://doi.org/10.1175/JCLI-D-14-00325.1

England, M., Polvani, L., & Sun, L. (2018). Contrasting the Antarctic and Arctic atmospheric responses to projected sea ice loss in the late twenty-first century. *Journal of Climate*, *31*(16), 6353–6370. https://doi.org/10.1175/JCLI-D-17-0666.1

Francis, J. a., & Vavrus, S. J. (2012). Evidence linking Arctic amplification to extreme weather in mid-latitudes. *Geophysical Research Letters*, *39*, L06801. https://doi.org/10.1029/2012GL051000

Gent, P. R., Danabasoglu, G., Donner, L. J., Holland, M. M., Hunke, E. C., Jayne, S. R., et al. (2011). The Community Climate System Model Version 4. *Journal of Climate*, *24*(19), 4973–4991. https://doi.org/10.1175/2011JCLI4083.1

Graversen, R. G., & Wang, M. (2009). Polar amplification in a coupled climate model with locked albedo. *Climate Dynamics*, *33*, 629–643. https://doi.org/10.1007/s00382-009-0535-6

Hay, S., Kushner, P., Blackport, R., & McCusker, K. (2018). On the relative robustness of the atmospheric circulation response to high-latitude and low-latitude warming. *Geophysical Research Letters*, *45*, 6232–6241. https://doi.org/10.1029/2018GL077294

Knutson T. (2003). FMS slab ocean model technical documentation, online at https://www.gfdl.noaa.gov/fms-slab-ocean-model-technical-documentation/.

Kretschmer, M., Coumou, D., Donges, J. F., & Runge, J. (2016). Using causal effect networks to analyze different Arctic drivers of midlatitude winter circulation. *Journal of Climate*, *29*(11), 4069–4081. https://doi.org/10.1175/JCLI-D-15-0654.1

Kug, J.-S., Jeong, J.-H., Jang, Y.-S., Kim, B.-M., Folland, C. K., Min, S.-K., & Son, S.-W. (2015). Two distinct influences of Arctic warming on cold winters over North America and East Asia. *Nature Geoscience*, *8*(10), 759–762. https://doi.org/10.1038/ngeo2517

Liu, W., Fedorov, A., & Sevellec, F. (2019). The mechanisms of the Atlantic meridional overturning circulation slowdown induced by Arctic sea ice decline. *Journal of Climate*, *32*(4), 977–996. https://doi.org/10.1175/JCLI-D-18-0231.1

Liu, W., & Fedorov, A. V. (2019). Global impacts of Arctic sea ice loss mediated by the Atlantic meridional overturning circulation. *Geophysical Research Letters*, *46*, 944–952. https://doi.org/10.1029/2018GL080602

McCusker, K. E., Fyfe, J. C., & Sigmond, M. (2016). Twenty-five winters of unexpected Eurasian cooling unlikely due to Arctic sea ice loss. *Nature Geoscience*, *9*, 838–842. https://doi.org/10.1038/ngeo2820

McCusker, K. E., Kushner, P. J., Fyfe, J. C., Sigmond, M., Kharin, V. V., & Bitz, C. M. (2017). Remarkable separability of circulation response to Arctic sea ice loss and greenhouse gas forcing. *Geophysical Research Letters*, *44*, 7955–7964. https://doi.org/10.1002/2017GL074327

Mori, M., Kosaka, Y., Watanabe, M., Nakamura, H., & Kimoto, M. (2019). A reconciled estimate of the influence of Arctic sea-ice loss on recent Eurasian cooling. *Nature Climate Change*, *9*, 123–129. https://doi.org/10.1038/s41558-018-0379-3

Mori, M., Watanabe, M., Shiogama, H., Inoue, J., & Kimoto, M. (2014). Robust arctic sea-ice influence on the frequent Eurasian cold winters in past decades. *Nature Geoscience*, *7*, 869–873. https://doi.org/10.1038/ngeo2277

Ogawa, F., Keenlyside, N., Gao, Y., Koenigk, T., Yang, S., Suo, L., et al. (2018). Evaluating impacts of recent Arctic sea ice loss on the Northern Hemisphere winter climate change. *Geophysical Research Letters*, *45*, 3255–3263. https://doi.org/10.1002/2017GL076502

Oudar, T., Sanchez-Gomez, E., Chauvin, F., Cattiaux, J., Terray, L., & Cassou, C. (2017). Respective roles of direct GHG radiative forcing and induced Arctic sea ice loss on the Northern Hemisphere atmospheric circulation. *Climate Dynamics*, *49*(11-12), 3693–3713. https://doi.org/10.1007/s00382-017-3541-0

Overland, J. E., Wood, K. R., & Wang, M. (2011). Warm Arctic-cold continents: Climate impacts of the newly open arctic sea. *Polar Research*, *30*(SUPPL.1), 1–14. http://doi.org/10.3402/polar.v30i0.15787

Peings, Y. (2019). Ural blocking as a driver of early-winter stratospheric warmings. *Geophysical Research Letters*, *46*, 5460–5468. https://doi.org/10.1029/2019GL082097

Perlwitz, J., Hoerling, M., & Dole, R. (2015). Arctic tropospheric warming: Causes and linkages to lower latitudes. *Journal of Climate*, *28*, 2154–2167. https://doi.org/10.1175/JCLI-D-14-00095.1

Scinocca, J. F., Reader, M. C., Plummer, D. A., Sigmond, M., Kushner, P. J., Shepherd, T. G., & Ravishankara, R. (2009). Impact of sudden Arctic sea-ice loss on stratospheric polar ozone. *Geophysical Research Letters*, *36*, L24701. https://doi.org/10.1029/2009GL041239

Screen, J. A., Deser, C., Smith, D. M., Zhang, X., Blackport, R., Kushner, P. J., et al. (2018). Consistency and discrepancy in the atmospheric response to Arctic sea-ice loss across climate models. *Nature Geoscience*, *11*(3), 155–163. https://doi.org/10.1038/s41561-018-0059-y

Smith, D. M., Dunstone, N. J., Scaife, A. A., Fiedler, E. K., Copsey, D., & Hardiman, S. C. (2017). Atmospheric response to Arctic and Antarctic sea ice: The importance of ocean–atmosphere coupling and the background state. *Journal of Climate*, *30*(12), 4547–4565. https://doi.org/10.1175/JCLI-D-16-0564.1

Smith, D. M., Screen, J. A., Deser, C., Cohen, J., Fyfe, J. C., García-Serrano, J., et al. (2019). The Polar Amplification Model Intercomparison Project (PAMIP) contribution to CMIP6: Investigating the causes and consequences of polar amplification. *Geoscientific Model Development*, *12*, 1139–1164. https://doi.org/10.5194/gmd-12-1139-2019

Stuecker, M. F., Bitz, C. M., Armour, K. C., Proistosescu, C., Kang, S. M., Xie, S. P., et al. (2018). Polar amplification dominated by local forcing and feedbacks. *Nature Climate Change*, *8*(12), 1076–1081. https://doi.org/10.1038/s41558-018-0339-y

Sun, L., Alexander, M. A., & Deser, C. (2018). Evolution of the global coupled climate response to Arctic sea ice loss during 1990–2090 and its contribution to climate change. *Journal of Climate*, *31*(19), 7823–7843. https://doi.org/10.1175/JCLI-D-18-0134.1

Sun, L., Deser, C., & Tomas, R. A. (2015). Mechanisms of stratospheric and tropospheric circulation response to projected Arctic sea ice loss. *Journal of Climate*, *28*(19), 7824–7845. https://doi.org/10.1175/JCLI-D-15-0169.1

Sun, L., Perlwitz, J., & Hoerling, M. (2016). What caused the recent "warm Arctic, cold continents" trend pattern in winter temperatures? *Geophysical Research Letters*, *43*, 5345–5352. https://doi.org/10.1002/2016GL069024

Tomas, R. A., Deser, C., & Sun, L. (2016). The role of ocean heat transport in the global climate response to projected arctic sea ice loss. *Journal of Climate*, *29*(19), 6841–6859. https://doi.org/10.1175/JCLI-D-15-0651.1

Wang, K., Deser, C., Sun, L., & Tomas, R. (2018). Fast response of the tropics to an abrupt loss of Arctic sea ice via ocean dynamics. *Geophysical Research Letters*, *45*, 4264–4272. https://doi.org/10.1029/2018GL077325

Winton, M. (2008). Sea ice-albedo feedback and nonlinear Arctic climate change. In *Arctic sea ice decline: Observations, projections, mechanisms, and implications*, *Geophys. Monogr.* (Vol. 180, pp. 111–131). Washington, DC: Amer. Geophys. Union. https://doi.org/10.1029/180GM09

Yoshimori, M., Abe-Ouchi, A., Tatebe, H., Nozawa, T., & Oka, A. (2018). The importance of ocean dynamical feedback for understanding the impact of mid-high latitude warming on tropical precipitation change. *Journal of Climate*, *31*(6), 2417–2434. https://doi.org/10.1175/JCLI-D-17-0402.1

Zwiers, F. W., & von Storch, H. (1995). Taking serial correlation into account in tests of the mean. *Journal of Climate*, *8*, 336–351. https://doi.org/10.1175/1520-0442(1995)008<0336:TSCIAI>2.0.CO;2